JPE 16-3-17

http://dx.doi.org/10.6113/JPE.2016.16.3.994
ISSN(Print): 1598-2092 / ISSN(Online): 2093-4718

Feed-Forward Approach in Stator-Flux-Oriented Direct Torque Control of Induction Motor with Space Vector Pulse-Width Modulation

Muhterem Özgür Kızılkaya† and Kayhan Gülez*

†Dept. of Electronic Eng., Turkish Air Force Academy, Istanbul, Turkey
*Dept. of Control and Automation Eng., Yıldız Technical University, Istanbul, Turkey

Abstract

Two major obstacles in the utilization of electrical vehicles are their price and range. The collaboration of direct torque control (DTC) with induction motor (IM) is preferred for its low cost, easy implementation, and parameter independency. However, in terms of edges, the method has drawbacks, such as variable switching frequency and undesired current harmonic distortion. These drawbacks result in acoustic noise, reduced efficiency, and electromagnetic interference. A feed-forward approach for stator-flux-oriented DTC with space vector pulse-width modulation is presented in in this paper. The outcome of the proposed method is low current harmonic distortion with fixed switching frequency while preserving the torque performance and simple application feature of basic DTC. The method is applicable to existing and forthcoming IM drive systems via software adaptation. The validity of the proposed method is confirmed by simulation and experimental results.

Key words: Direct torque control, Feed-forward control, Flux linkage ripple, Space vector pulse-width modulation

NOMENCLATURE

ψ	Flux linkage
θ	Angle of flux linkage vector
V	Voltage
i	Current
r	Resistance
L	Inductance
L_m	Mutual inductance between stator and rotor
w	Angular speed
γ	Load angle
P	Number of poles
σ	Leakage factor
T	Torque
μ	Proportional compensation factor
V_ψ, V_T	Horizontal and vertical voltage vectors

SUBSCRIPTS

s,r	Stator and rotor quantities
a,b,c	phases a, b, and c
D,Q	D and Q axes

Manuscript received Oct. 9, 2015; accepted Jan. 6, 2016
Recommended for publication by Associate Editor Gaolin Wang.
†Corresponding Author: mkizilkaya@hho.edu.tr
Tel: +90-212 6632490 - 4345, Turkish Air Force Academy
*Department of Control and Automation, Yıldız Technical University Turkey

I. INTRODUCTION

Induction motor (IM) and interior permanent magnet synchronous motor (IPMSM) have been utilized as the main traction system by commercial electric vehicle (EV) companies in the last decade [1]-[3]. IPMSM has high efficiency [4], [5], and IM is inexpensive and reliable. Furthermore, the perfomance of IM, with appropriate control strategies, is comparable with that of costly permanent magnet alternatives; hence, it is a good candidate for low-cost EV production [6], [7].

The direct torque control (DTC) method has been extensively applied in many industrial fields since its invention [8], [9] because of its fast and precise control response [10], [11]. However, varying switching frequency, torque ripple, and current harmonics are the drawbacks of this method [12], [13]. Undesired current harmonics result in

acoustic noise and electromagnetic interference (EMI) problems [14]. Costly and large active or passive filters are required to attenuate the troublesome current harmonics and EMI in a wide band spectrum [15], [16].

Feed-forward controller is a favorable method to eliminate disturbance [17], [18]. This method is also effective in exactly controlling complicated systems with simple models, as performed in [19]. This method is preferred to increase the control performance of simple control techniques, such as proportional–integral (PI) controller [20] or phase-locked loop method [21]. In this study, a simple torque model of IM is built to ensure that the complexity of all the systems does not increase. A feed-forward controller matched with a proportional controller is utilized to determine the voltage vectors of DTC with space vector pulse-width modulation (SVPWM).

SVPWM-based DTC is a popular method to reduce current ripple and overcome the variable switching frequency problem [22], [23]. Any voltage vector with intended amplitude and angle can basically be generated by using available voltage vectors with SVPWM [24]. The difference between the applications is in the determination of appropriate voltage vectors and their duration. Satheesh et al. and Bassem et al. utilized different SVPWM-based DTC methods to overcome the variable switching frequency problem in [25], [26]. Kenny et al. used the deadbeat control method to obtain the appropriate voltage vector and applied SVPWM to generate it at the cost of increased complexity [27]. Lai and Chen employed two PI controllers separately to determine the voltage vector components for flux linkage and torque generation and applied them with SVPWM. The PI controllers slowed down the torque response of the overall system [28]. Rashag et al. utilized a fuzzy logic controller instead of PI regulators to accelerate the process of determining the voltage vectors at the input of the SVPWM module [29]. Using a sliding-mode controller instead of a PI controller at the input of SVPWM is another option, as shown in [30]. Both method increase the torque performance of the system by utilizing a highly complicated controller instead of a PI regulator. Tang et al. utilized a modified SVPWM cycle to reduce torque and flux ripple at the cost of increased switching frequency. However, the method was not verified by the experimental results [31]. Discrete SVPWM can also be used to reduce the torque and current ripple in DTC-driven IM drives, as shown in [32]. All these methods are effective in reducing current ripple, but they require additional computational effort and violate the simplicity or motor parameter independency of the DTC algorithm. The advantage of the proposed method over these discussed ones is the use of basic DTC topology and its simple algorithm; moreover, no additional parameters are required

The basic DTC method compares the reference and estimated torque and stator flux linkage magnitudes to determine the optimum voltage vector to be applied. Torque and flux linkage estimation is performed with the measured voltage and phase current by using a voltage-model-based method [13]. A basic DTC scheme for EV applications with IM is shown in Fig. 1 [33].

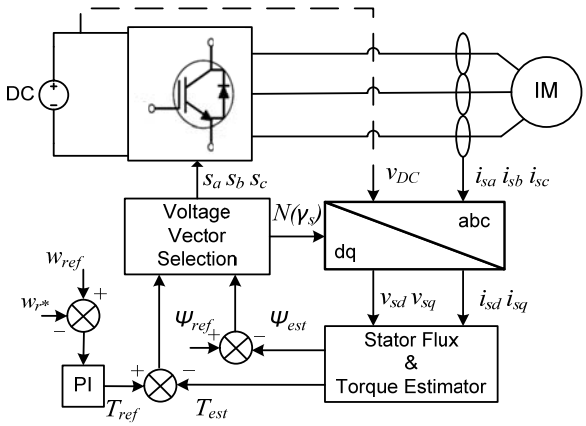

Fig. 1. Basic DTC configuration for EV applications.

Most studies mainly focused on the torque performance of a system, and flux linkage ripple and current harmonics are regarded as second priorities only.

The main consideration of this study is to reduce current harmonic by smoothly rotating the stator flux linkage vector without any degradation of the torque performance of the basic DTC. A feed-forward controller is applied via the mean value of the measured voltage vector that is assigned for torque generation. A proportional controller is included to reduce the torque error while preserving the fast torque response characteristic. The proposed method is applicable to SVPWM that uses fixed switching frequency, thus leading to the possible usage of small and affordable line filters in the system. The voltage vectors of SVPWM and their interval are determined by calculating the magnitude of the horizontal and vertical voltage vector components assigned to flux linkage and torque generation, respectively. The controller is explained in detail in Section III.

A comparison of the proposed approach with the basic DTC scheme is presented. The simulation and experimental results reveal reduced flux and current ripple with low current harmonics at low and rated speed values. Simulation and experimental verification are performed for the basic DTC scheme and hardware, as shown in Fig. 1. Their results also indicate that the proposed method is applicable to existing and forthcoming DTC drive system topologies.

II. Operation Theory

DTC is an advanced method to retain IM torque and stator flux linkage parameters inside the control intervals by applying an appropriate voltage vector from six active and two zero vectors in a stationary DQ frame, as shown in Fig. 2.

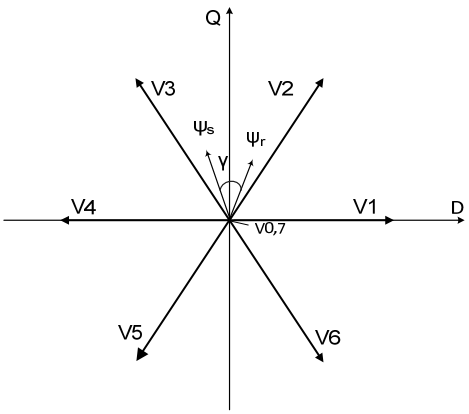

Fig. 2. Voltage vectors of IM in a stationary DQ frame.

In the stationary reference frame, where the D axis is attached on the stator winding of phase A, the stator and rotor voltage equations of IM are provided as Equs. (1) and (2) [28].

$$\frac{d}{dt}\overline{\psi_s} = \overline{V_s} - r_s\overline{I_s} \tag{1}$$

$$\frac{d}{dt}\overline{\psi_r} = \overline{V_r} - r_r\overline{I_r} + jw_r\overline{\psi_r} \tag{2}$$

For squirrel cage IM, the rotor voltage "V_r" is zero. Stator voltage and current vector can be handled by two voltage and two current sensor measurements [33]. The voltage and current magnitudes in the DQ frame can be determined for a wye-connected squirrel cage IM, as indicated in Equs. (3) to (8).

$$i_{sa} + i_{sb} + i_{sc} = 0 \tag{3}$$

$$v_{sa} + v_{sb} + v_{sc} = 0 \tag{4}$$

$$i_{sD} = i_{sa} \tag{5}$$

$$i_{sQ} = \frac{i_{sa} + 2i_{sb}}{\sqrt{3}} \tag{6}$$

$$v_{sD} = \frac{1}{3}(v_{ba} - v_{ac}) \tag{7}$$

$$v_{sQ} = \frac{-1}{\sqrt{3}}(v_{ba} + v_{ac}) \tag{8}$$

The stator flux linkage vector in DQ frame Ψ_{sD} / Ψ_{sQ} and generated torque T_{est} are estimated with Equs. (9) to (12), as performed in [34].

$$\psi_{sD} = \int (V_{sD} - r_s I_{sD})dt \tag{9}$$

$$\psi_{sQ} = \int (V_{sQ} - r_s I_{sQ})dt \tag{10}$$

$$\theta = \arctan\frac{\psi_{sD}}{\psi_{sQ}} \tag{11}$$

$$T_{est} = \frac{3P}{4}((\psi_{sD} i_{sQ}) - (\psi_{sQ} i_{sD})) \tag{12}$$

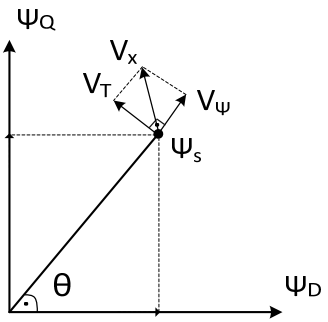

Fig. 3. Stator flux linkage, horizontal, and vertical voltage vectors.

III. Proposed Method

The instantaneous stator flux linkage vector can be represented in a stationary reference frame by its magnitude $|\psi_s|$ and angle Θ, as presented in Fig. 3. The voltage vector to be applied, V_x, can be decomposed into horizontal and vertical components with respect to the flux linkage vector to control the flux linkage magnitude and electromechanical torque, respectively, as defined in Equ. (13).

$$\overrightarrow{V_x} = \overrightarrow{V_T} + \overrightarrow{V_\psi} \tag{13}$$

The horizontal voltage vector component "V_ψ" is associated with stator flux linkage magnitude, and the vertical voltage vector component V_T is associated with electromechanical torque, as explained in [20].

The magnitude of stator flux linkage vector Ψ_s is a slowly varying parameter; it can be maintained within a small bandwidth (Equ. (14)) by using an adequate control strategy, in which the resistive voltage drop by the stator current in Equ. (1) is neglected.

$$\frac{d}{dt}|\psi_s| = V_\psi \tag{14}$$

Controlling the stator flux linkage magnitude causes the rotor flux linkage magnitude to exhibit a small variation, as explained in Equs. (1) and (2) [35]; thus, the electromechanical torque output can be controlled by load angle (Equ. (15)).

$$T_e = \frac{3}{2}P\frac{L_m}{\sigma L_s L_r}\psi_s\psi_r \sin\gamma \tag{15}$$

The rate of change in the torque output with respect to time is derived from Equ. (15) and shown in Equ. (16).

$$\frac{dT_e}{dt} = \frac{3}{2}P\frac{L_m}{\sigma L_s L_r}\psi_s\psi_r \cos\gamma\frac{d\gamma}{dt} \tag{16}$$

The variation in load angle is a result of the difference between the angular speeds of stator and rotor flux linkage vectors, as depicted in Fig. 4. To increase torque at the motor output via load angle, vertical voltage vector component V_T is applied to the motor windings in the counter clockwise direction for the related counter clockwise operation at a

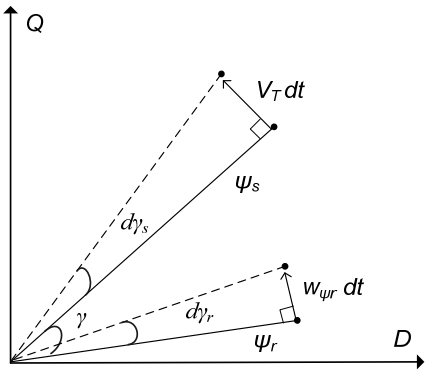

Fig. 4. Stator and rotor flux linkages, variation in load angle by the vertical voltage vector, and rotation of the rotor flux linkage.

magnitude that maintains the angular speed of the stator flux linkage vector faster than the angular speed of the rotor flux linkage vector. To decrease torque at the motor output, vertical voltage vector component V_T is also applied so that the angular speed of the stator flux linkage vector becomes slower than the angular speed of the rotor flux linkage vector.

Stator flux linkage angular speed is a result of the vertical voltage vector, and rotor flux linkage rotational speed $w_{\psi r}$ is a function of rotor speed and time constant between the stator and rotor flux linkages.

Any sufficiently small angle magnitude can be expressed as its sine value (Equ. (17)).

$$\gamma \approx \sin(\gamma) : \gamma << 1 \tag{17}$$

The variation in load angle can be determined by subtracting the variation in stator and rotor flux linkage angles (Equs. (18) to (21)).

$$d\gamma = d\gamma_s - d\gamma_r \tag{18}$$

$$d\gamma_s = \frac{V_T dt}{\sqrt{((V_T dt)^2 + (\psi_s)^2}} \approx \frac{V_T dt}{\psi_s} \tag{19}$$

$$d\gamma_r = \frac{w_{\psi r} dt}{\sqrt{((w_{\psi r})^2 + (\psi_r)^2}} \approx \frac{w_{\psi r} dt}{\psi_r} \tag{20}$$

$$\frac{d\gamma}{dt} \approx \left(\frac{V_T}{\psi_s} - \frac{w_{\psi r}}{\psi_r} \right) \tag{21}$$

Equ. (21) indicates that load angle can be controlled by the vertical voltage vector for an operation point defined as constant rotor speed and stator flux linkage magnitude. Therefore, vertical voltage vector V_T exists; it indicates that load angle and motor torque output variation are zero. In applications, torque and applied voltage magnitude have ripples because the required voltage is generated as the sum of two sequential voltage vectors; thus, the mean values of variables are preferred instead of instantaneous values for modeling. Torque generation of IM by the applied voltage vector can be modeled with a first-order equation (Equ. (22)). The assumption is as follows: at any operation point, the mean value of the applied vertical voltage vector is associated with the mean value of the output torque. The calculation of k for any operating point is the core of this study.

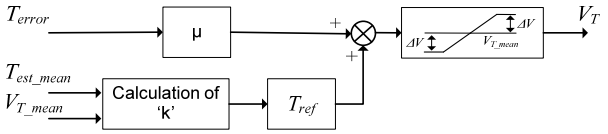

Fig. 5. Block diagram of the proposed controller.

$$V_{T-mean} = k * T_{est-mean}, \tag{22}$$

where $V_{T\text{-}mean}$ and $T_{est\text{-}mean}$ are the mean values of the vertical voltage vector and the estimated electromechanical torque, respectively. For any operating point, the required vertical voltage vector to generate the reference torque output can be estimated via the k value calculated in the previous step.

The torque error in the control system is the difference between the reference and estimated torques in Equ. (23).

$$T_{error} = T_{ref} - T_{est} \tag{23}$$

The control law, as depicted by Equs. (24) and (25), aims to estimate the magnitude of the vertical voltage vector to generate the reference torque output.

$$V_T = T_{ref} \cdot \left(\frac{V_{T-mean}}{T_{est-mean}}\right) + \mu\left(\frac{V_{T-mean} \cdot T_{error}}{T_{est-mean}}\right), \tag{24}$$

$$(V_{T-mean} + \Delta V) > V_T > (V_{T-mean} - \Delta V), \tag{25}$$

where T_{ref} and T_{est} are the reference and estimated torque values, respectively. The first part of Equ. (24) estimates the required vertical voltage vector using the first-order torque model by calculating the k value with torque errors as a consequence of using a simple model (Equ. (22)). A proportional compensation factor (μ) is added to the control law in a second part to compensate for the torque errors. The control algorithm keeps the vertical voltage within a band of $2\Delta V$ around the mean value of the applied vertical voltage vector to attenuate the current harmonic (Equ. (25)). The controller is shown in Fig. 5.

Torque reference is used to calculate the vertical voltage vector via the torque model through the feed-forward approach and the torque error with a proportional controller. The horizontal voltage vector is determined by Equ. (14).

The calculated vertical and horizontal voltage vectors are transformed to VD and VQ in the stationary stator axis through the transformation matrix shown in Fig. 3 via Equ. (26).

$$\begin{bmatrix} V_D \\ V_Q \end{bmatrix} = \begin{bmatrix} \sin\theta & \cos\theta \\ \cos\theta & \sin\theta \end{bmatrix} x \begin{bmatrix} V_T \\ V_\Psi \end{bmatrix} \tag{26}$$

Moreover, Park transformation [13] is applied to calculate the components of three-phase voltage vectors, and SVPWM is applied to generate the calculated voltage vectors for the drive system.

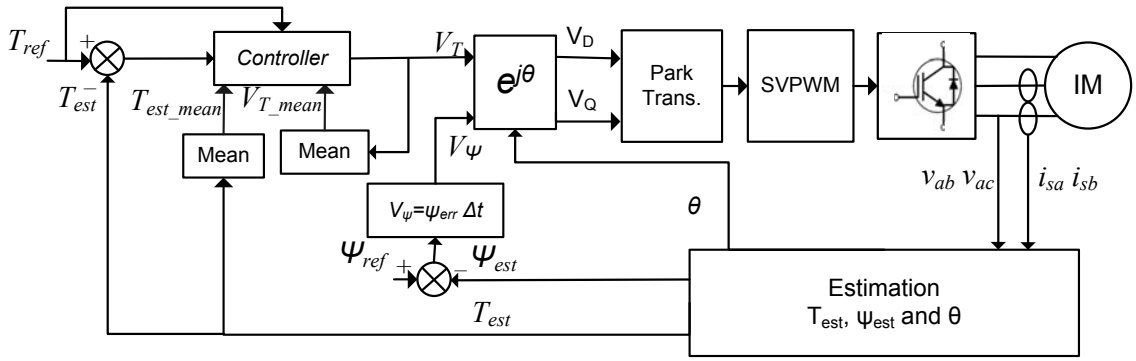

Fig. 6. Block diagram of the proposed DTC method.

TABLE I
MOTOR PARAMETERS

Motor type	Squirrel Cage IM
Stator resistance	12.1 Ω
Stator inductance	10.74 mH
Rotor inductance	10.74 mH
Mutual inductance	203.7 mH
Pole pair	3
Inertia	0.00254 kgm^2
Rated speed	925 rpm
Rated power	750 W
Operation voltage	230/400 V
Rated current (wye connected)	2.1 A
Rated torque (wye connected)	4.46 Nm
Rated startup torque (wye connected)	2.1 Nm

IV. SIMULATION STUDY

The proposed method is applied to a particular case to verify its effectiveness. A simulation is implemented in the Simulink environment by using the block diagram shown in Fig. 6.

Phase voltage and current measurement blocks are utilized for torque and flux linkage vector estimations with Equs. (3) to (12). The estimated torque and flux linkage are compared with the reference ones. Horizontal voltage vector $V\psi$ is calculated with Equ. (14). Vertical voltage vector VT is calculated with the controller depicted in Fig. 5. The calculated vertical and horizontal voltage vectors are transformed into a stationary frame that is appropriate for SVPWM.

The parameters of the test motor measured and adopted in the simulation are provided in Table I.

A square wave torque reference signal of 1 Hz 4.5 Nm is applied to evaluate the effectiveness of the proposed method. Figs. 7(a) and 7(b) show the electromechanical torque output for the basic DTC and the proposed method, respectively. Torque output has a set bandwidth for the basic method, whereas the bandwidth for the proposed method is determined by motor operating point and switching frequency. The switching cycle Δt for SVPWM is set to 2 ms to make the switching frequency 5 kHz for the simulations. The

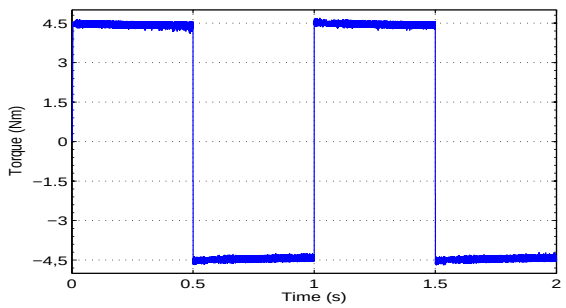

(a)

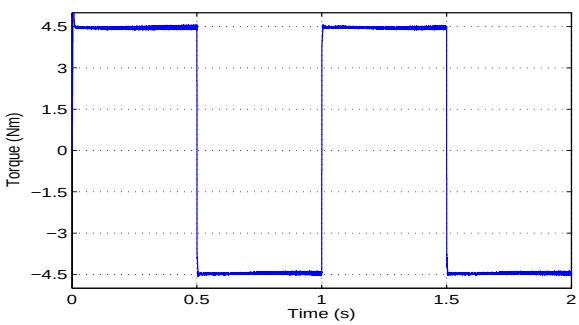

(b)

Fig. 7. Torque output of (a) basic DTC and (b) the proposed method.

switching frequency of the basic DTC varies between 3 and 6 kHz. The fast torque response property of the basic DTC method is preserved in the proposed method.

An efficient operating point for the test motor by stator flux linkage is approximately 0.5 Wb. The flux linkage reference value is set to 0.5 Wb for the simulation and experimental verification tests. Fig. 8 shows the flux linkage outputs for the basic DTC and the proposed method.

The basic DTC method requires 17 ms to settle at startup and 35 ms when the torque reference is shifted. The flux linkage ripple is higher than that of the proposed method. The proposed method requires only 6 ms settling time at startup. Its flux linkage ripple increases with speed as a result of the fixed switching frequency but is still lower than that of the basic DTC at steady state (Table II).

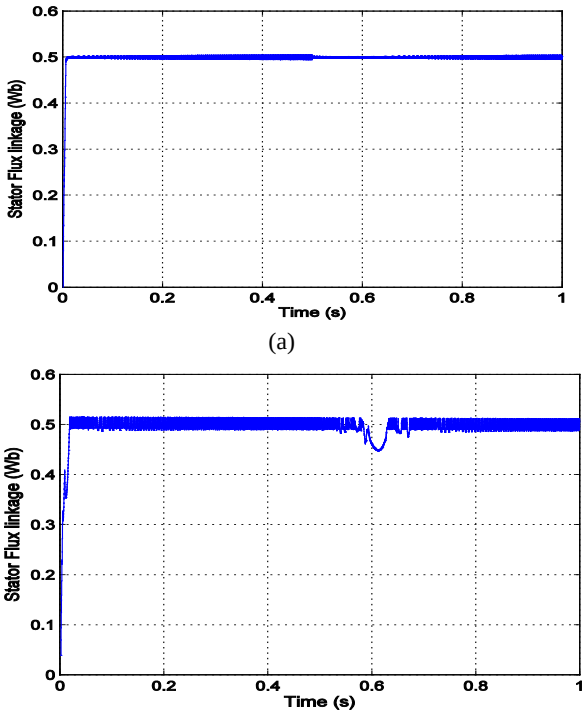

Fig. 8. Simulated flux linkage waveform of (a) basic DTC and (b) the proposed method during torque tests.

TABLE II
FLUX LINKAGE RIPPLE FROM THE SIMULATION RESULTS

	Basic DTC	Proposed Method
Transient	10.6%	2.0%
Steady state	4.54%	2.0%

The deviation from the reference is used in ripple computation. Steady state and transient ripple are similar for the proposed method because no priority exists between torque and flux linkage in the control law.

The improvement in flux linkage ripple leads to a reduction of the total harmonic distortion for the phase current of IM. The phase current and frequency spectrum for the rated speed under rated load are depicted in Figs. 9(a) to 9(d) for DTC and the proposed method.

The total harmonic distortion value is 11.91% for the basic DTC and 4.86% for the proposed method. The harmonic content of the basic DTC spreads in a wide spectrum, whereas it is centered around the multiples of switching frequency in the proposed method, which makes it beneficial for filter design.

The vertical voltage vector is crucial in the torque response of the system via the proposed method. The vertical vector magnitude while the torque reference is shifted between 4.5 and −4.5 Nm is depicted in Fig. 10. The vertical voltage vector is increased by the rotor speed in a predetermined band.

The calculation of the k value is the core of the proposed method. At startup, the prediction of k is not viable until the motor stator flux linkage value reaches the set value. Afterward, the k value exhibits a smooth change for the constant torque reference. When the torque reference is shifted, the k value is updated for the new operating point, which results in a sudden change in the k value, as shown in Fig. 11.

The torque performance of the proposed method is also assessed by means of a city drive cycle on an imaginary

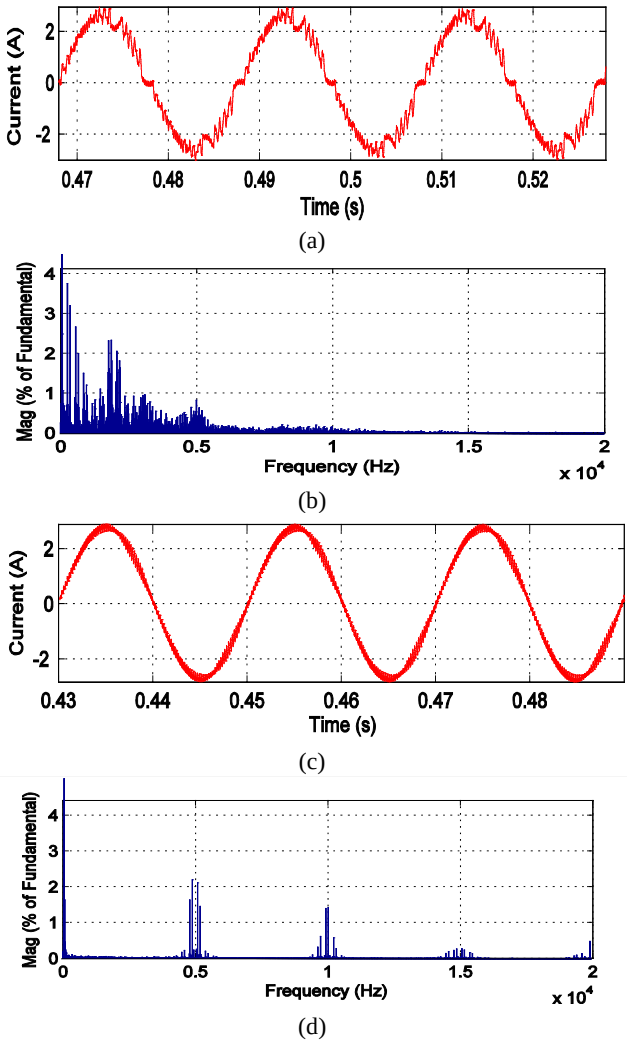

Fig. 9. Phase current and harmonic distortion for basic DTC and the proposed method from top to bottom (a) to (d).

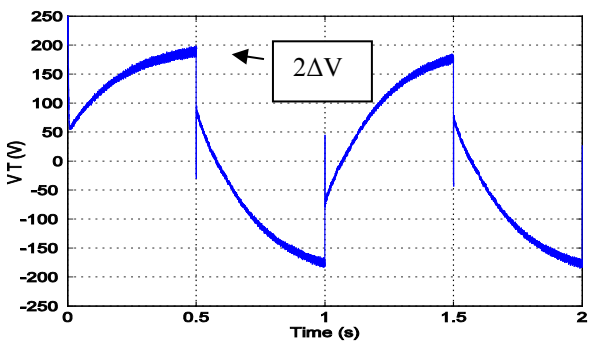

Fig. 10. Vertical voltage vector while the torque reference is shifted between 4.5 and −4.5 Nm.

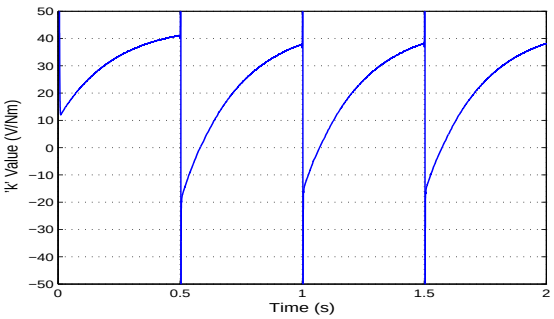

Fig. 11. Calculated k parameter while the torque reference is shifted between 4.5 and −4.5 Nm.

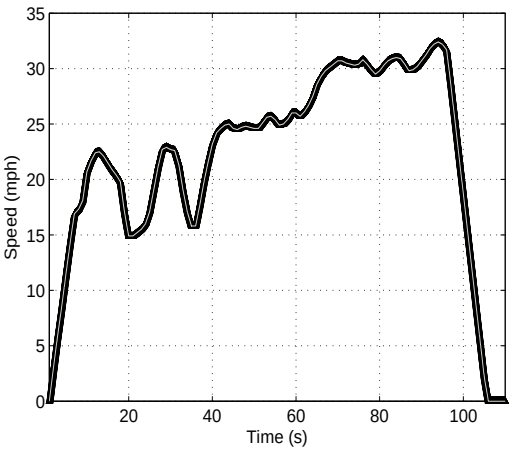

Fig. 12. Speed-tracking performance over a city drive cycle. Reference speed data are presented by the gray line, and the performed one is the black line.

TABLE III
ELECTRIC MOTORCYCLE KINEMATICS

Vehicle and payload mass	100 kg
Gear ratio	4
Wheel radius	20 cm
Wheel inertia	1 m^2
Vehicle frontal area	0.1 kgm^2
Rolling resistance coefficient	0.0267
Road gradient	0

electric motorcycle, as depicted in Fig. 12. The vehicle dynamics of an electric motorcycle are utilized to determine the torque requirement [36]. A PI controller is inserted into the block diagram in Fig. 6, as in Fig. 1, to track the speed reference.

The kinematics of the electric motorcycle are shown in Table III.

V. EXPERIMENTAL VERIFICATION

A wye-connected experimental IM drive system (shown in Fig. 13) is built in the laboratory to verify the proposed DTC scheme experimentally.

The setup is designed as a basic DTC drive system topology

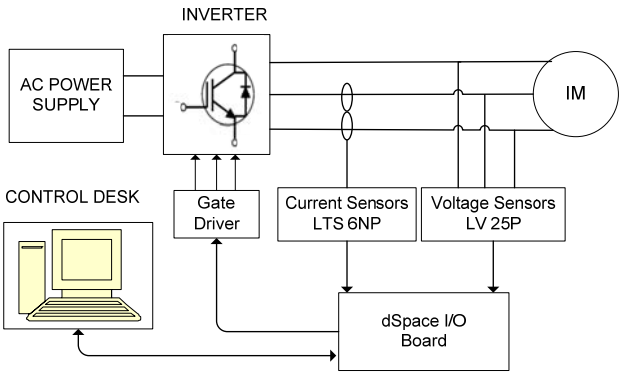

Fig. 13. Experimental setup.

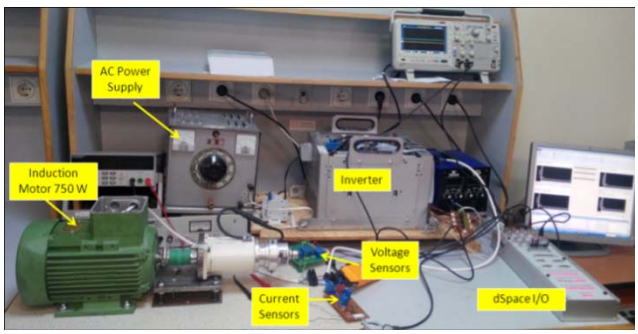

Fig. 14. Test setup used for basic DTC and the proposed method.

and used for both basic DTC and the proposed method to observe the distinction.

DTC software is developed in the Simulink environment, and a dSpace 1104 controller board is utilized to implement the real-time algorithm. The motor is driven by a six-switch insulated-gate bipolar transistor bridge inverter. The SVPWM frequency is set to 1 kHz during the tests. Phase voltages and currents are measured with sensors to estimate the electromechanical torque and flux linkage. The test setup is shown in Fig. 14.

The test results are obtained either by oscilloscope measurements or calculated variables handled via the dSpace I/O board. Harmonic analysis is accomplished with measured and recorded data files.

The main advantage of the proposed method over basic DTC is the reduced flux linkage ripple. The flux linkage reference is set to 0.5 Wb and estimated with the low-pass filter method. A step change in torque reference is applied to observe both transient- and steady-state flux linkage outputs for both methods, as shown in Figs. 15(a) and (b), respectively.

The flux linkage ripple data for both situations are shown in Table IV. The proposed method has low ripple for both steady and transient states. The flux linkage output is unaffected by the step change in the torque output, but the basic DTC requires 60 ms to settle.

The improvement in flux linkage ripple results in a low harmonic content in phase current in the steady state at low and rated speed operations, as depicted in Figs. 16 and 17. The phase current of the proposed method is close to a sinus

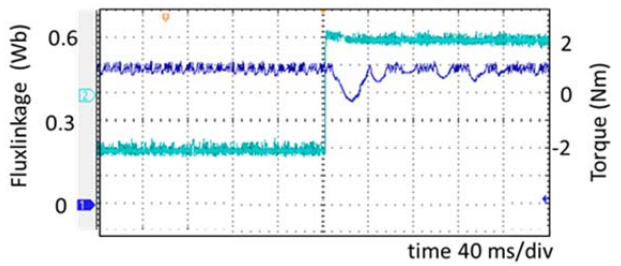

(a)

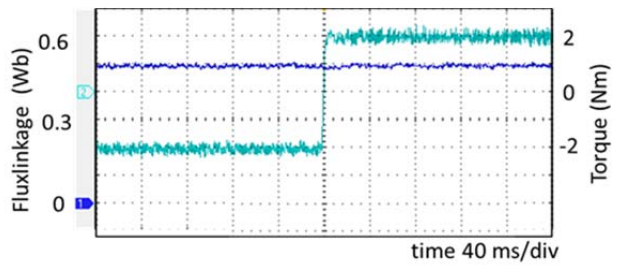

(b)

Fig. 15. Stator flux linkage when the torque reference is changed for (a) basic DTC and (b) the proposed method. Flux linkage is presented by the blue line, and torque is denoted by the green line.

TABLE IV
FLUX LINKAGE RIPPLE FOR THE EXPERIMENTAL RESULTS

	Basic DTC	Proposed Method
Steady state	9%	4%
Transient	23%	4%

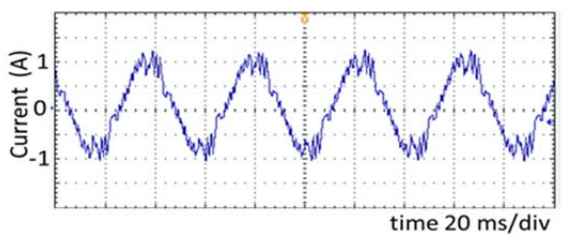

(a)

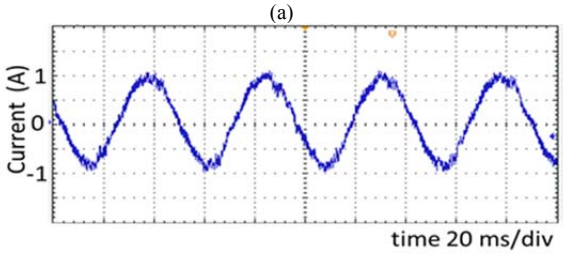

(b)

Fig. 16. Phase current at 400 rpm for (a) basic DTC and (b) the proposed method.

shape, as observed in the oscilloscope measurement. The total harmonic distortion values are 14.1% and 6.3% at low speed and 19.6% and 9.07% at rated speed for basic DTC and the proposed method, respectively.

The horizontal and vertical voltage vectors are controlled separately. The vertical voltage needs to be increased to generate constant torque as the motor speed increases; the same condition applies to the reverse rotation. Torque

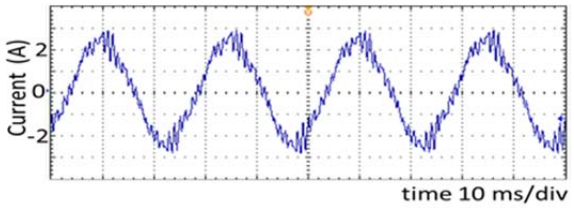

(a)

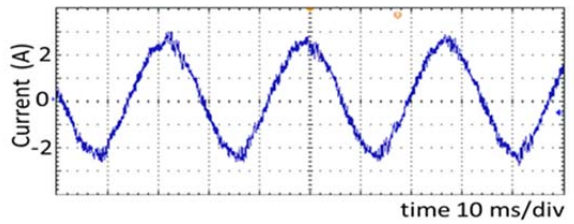

(b)

Fig. 17. Phase current at 900 rpm for (a) basic DTC and (b) the proposed method.

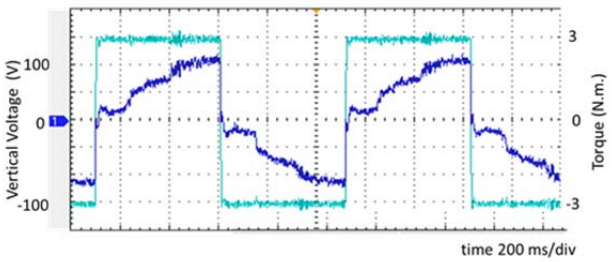

Fig. 18. Estimated torque and applied vertical voltage vector. Vertical voltage is presented by the blue line, and torque is denoted by the green line.

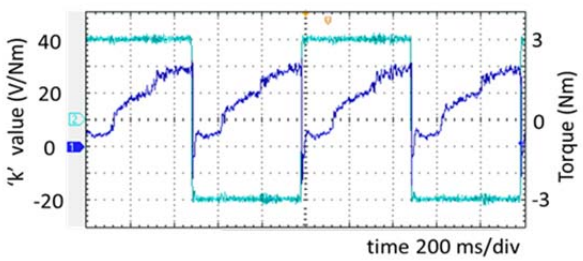

Fig. 19. Estimated torque and calculated "k" parameter. The "k" value is presented by the blue line, and torque is denoted by the green line.

reference is shifted between 3 and −3 Nm to observe the variation in the vertical voltage vector in both directions. Fig 18 shows the vertical voltage vector magnitude and torque output synchronously.

The estimated torque and applied vertical voltage vector, which are depicted in Fig. 19, are required to calculate the *k* value that is defined in this study by Equ. (22). Fig. 19 shows the *k* value and estimated torque.

Contrary to basic DTC, the proposed method controls the torque output and flux linkage separately. The required voltage vector and its duration are calculated in a stationary DQ frame via a novel approach and applied to a drive system by SVPWM. Improvements in the flux linkage ripple and phase current harmonic distortion are observed from the

simulation and experimental results. Furthermore, the fast torque response of the basic DTC is preserved.

VI. CONCLUSION

This paper presents a feed-forward approach with a proportional regulator for stator-flux-oriented DTC with SVPWM having low current harmonic distortion while preserving the simple application and fast torque response property of basic DTC. The proposed approach exhibits good performance by means of flux regulation with fixed switching frequency, which results in reduced phase current harmonics. This approach also has the advantages of simplicity for the filter design and flexible selection of the switching elements in the inverter. Another advantage of the proposed method is its applicability to current motor drive systems with software adaptation. The proposed method neither requires motor parameters, except stator resistance, nor complicated algorithms. Hence, it is a good candidate for the online selection of voltage vectors in the DTC of IM for current and future low-cost EV applications. The simulation and experimental results confirm the effectiveness of the proposed method.

ACKNOWLEDGMENT

This research is supported by the Turkish Air Force Academy in cooperation with the Yıldız Technical University Scientific Research Projects Coordination Department (Project Number: 2013-04-04 KAP01).

REFERENCES

[1] G. Pellegrino, A. Vagati, B. Boazzo, and P. Guglielmi, "Comparison of induction and PM synchronous motor drives for EV application including design examples," *IEEE Trans. Ind. Appl.*, Vol.48, No.6, pp.2322-2332, Nov./Dec. 2012.

[2] S. Rind, R. Yaxing, and L. Jiang, "Traction motors and speed estimation techniques for sensorless control of electric vehicles: a review,"*49th International Universities Power Engineering Conference (UPEC)*, pp. 1-6, Sep. 2014.

[3] A. Ghaderi, T. Umeno, and S. Masaru "A novel seamless direct torque control for electric drive vehicles," *Journal of Power Electronics*, Vol. 11, No. 4, pp. 449-455 Jul. 2011.

[4] A. A. Adam, K. Gulez, I. Aliskan, Y. Altun, R. Guclu, and M. Metin, "Steering DTC algorithm for IPMSM used in electrical vehicle with fast response and minimum torque ripple," *11th IEEE International Workshop on Advanced Motion Control*, pp. 279-283, Mar. 2010.

[5] T. D. Do, H. H. Choi, and J. Jung, "Nonlinear optimal DTC design and stability analysis for interior permanent magnet synchronous motor drives," *IEEE/ASME Trans. Mechatron.*, Vol.20, No.6, pp. 2716-2725, Dec. 2015.

[6] V. T. Buyukdegirmenci, A. M. Bazzi, and P. T. Krein, "Evaluation of induction and permanent-magnet synchronous machines using drive-cycle energy and loss minimization in traction applications," *IEEE Trans. Ind. Appl.,* Vol. 50, No. 1, pp. 395-403, Jan./Feb. 2014.

[7] J. Yu, W. Pei, and C. Zhang, "A loss-minimization port-controlled hamilton scheme of induction motor for electric vehicles," *IEEE/ASME Trans. M0echatron.*, Vol. 20, No. 6, pp. 2645-2653, Dec. 2015.

[8] I. Takahashi and T. Noguchi, "A new quick-response and high-efficiency control strategy of induction motor," *IEEE Trans. Ind. Appl.,*Vol. 22, No. 5, pp 820-827, Sep. 1986.

[9] M. Depenbrock, "Direct self-control (DSC) of inverter-fed induction machine," *IEEE Trans. Power Electron.*, Vol. 3, No. 4, pp. 420-429, Oct. 1988.

[10] T. Sutikno, N. Idris, and A. Jidin, "A review of direct torque control of induction motors for sustainable reliability and energy efficient drives," *Renewable and Sustainable Energy Reviews*, Vol. 32, pp. 548-558, Apr. 2014.

[11] S. A. Zaid, O. A. Mahgoub, and K. A. El-Metwally, "Implementation of a new fast direct torque control algorithm for induction motor drives," *IET Electric Power Appl.*, Vol. 4, No. 5, pp. 305-313, May 2010.

[12] B. Singh, S. Jain, and S. Dwivedi, "Torque ripple reduction technique with improved flux response for a direct torque control induction motor drive," *IET Power Electron.,* Vol. 6, No. 2, pp. 326-342, Feb. 2013.

[13] G. S. Buja and M. P.Kazmierkowski, "Direct torque control of PWM inverter-fed AC motors - a survey," *IEEE Trans. Ind. Electron.,* Vol. 51, No. 4, pp. 744-757, Aug. 2004.

[14] L. Xu, Z. Q. Zhu, and D. Howe, "Acoustic noise radiated from direct torque controlled induction motor drives," *IEEE Proc. Electric Power Applications*, Vol. 147, No. 6, pp. 491-496, Nov. 2000.

[15] D. A. Rendusara and P. N. Enjeti, "An improved inverter output filter configuration reduces common and differential modes dv/dt at the motor terminals in PWM drive systems," *IEEE Trans. Power Electron.,* Vol. 13, No. 6, pp. 1135-1143, Nov. 1998.

[16] A. A. Adam and K. Gulez, "Reduction of torque pulsation and noises in PMSM with hybrid filter topology," *Simulation Modelling Practice and Theory,* Vol. 19, No. 1, pp. 350-361, Jan. 2011.

[17] S. Ning, S. Zheng, and X. Wang, "The active disturbance rejection control with feed-forward compensation for hydraulic pump controlled motor speed system," *Fifth International Conference on Intelligent Control and Information Processing (ICICIP)*, pp.144-150, Aug. 2014.

[18] A. Baratam, A. M. Karlapudy, and S. Munagala, "Implementation of thrust ripple reduction for a permanent magnet linear synchronous motor using an adaptive feed forward controller," *Journal of Power Electronics*, Vol. 14, No. 4, pp. 687-694, Jul. 2014.

[19] S. J. Imen and M. Shakeri, "Feed forward adaptive control of a linear brushless DC motor," *Annual Conference in SICE*, pp. 2200-2204, Sep. 2007.

[20] B. Purwahyudi, H. S. Soebagio, M. Ashari, and T. Hiyama, "Feed-forward neural network for direct torque control of induction motor," *International Journal of Innovative Computing, Information and Control,* Vol. 7, No. 11, pp. 6135-6145, Nov. 2011.

[21] H. Machida, M. Kambara, K. Tanaka, and F. Kobayashi, "A motor speed control system using a hybrid of dual-loop PLL and feed-forward,"*11th IEEE International Workshop on Advanced Motion Control*, pp.185-190, Mar. 2010.

[22] T.G. Habetler, F. Profumo, M. Pastorelli, and L.M. Tolbert, "Direct torque control of induction machines using space vector modulation," *IEEE Trans. Ind. Appl.*, Vol. 28, No. 5, pp. 1045-1053, Sep./Oct. 1992.

[23] S. S. Sebtahmadi, H. Pirasteh, S. H. A. Kaboli, A. Radan, and S. Mekhilef, "A 12-Sector space vector switching scheme for performance improvement of matrix-converter based DTC of IM drive," *IEEE Trans. Power Electron.*, Vol. 30, No. 7, pp. 3804-3817, Jul. 2015.

[24] K. M. Kwon, J. M. Lee, J. M. Lee, and J. Choi, "SVPWM overmodulation scheme of three-level inverters for vector controlled induction motor drives," *Journal of Power Electronics*, Vol. 9, No. 3, pp. 481-490, Jul. 2009.

[25] G. Satheesh, T. R. Bramhananda, and B. Sai, "A novel space vector PWM based direct torque control algorithm for open end winding induction motor drive" *International Review of Automatic Control*, Vol. 6 No. 1, pp. 29, Jan. 2013.

[26] E.B. Bassem, G. Abdessattar, and M. Ahmed, "On the comparison between different space vector PWM strategies implemented in FSTPI-fed induction motor drives," *COMPEL,* Vol. 26, No. 1, pp.127-147, Jan. 2007.

[27] B. H. Kenny and R. D. Lorenz, "Stator and rotor flux based deadbeat direct torque control of induction machines," *IEEE Industry Applications Conference*, Vol. 1, pp. 133-139, Sep./Oct. 2001.

[28] Y.-S. Lai and J.-H. Chen, "A new approach to direct torque control of induction motor drives for constant inverter switching frequency and torque ripple reduction," *IEEE Trans. Energy Convers.*, Vol. 16, No. 3, pp. 220-227, Sep. 2001.

[29] H. F. Rashag, S. P. Koh, A. N. Abdalla, N. M. L. Tan, and K. H. Chong, "Modified direct torque control using algorithm control of stator flux estimation and space vector modulation based on fuzzy logic control for achieving high performance from induction motors," *Journal of Power Electronics*, Vol. 13, No. 3,pp. 369-380, May 2013.

[30] L. Tang, L Zhong, M. F. Rahman, and Y. Hu, "An investigation of a modified direct torque control strategy for flux and torque ripple reduction for induction machine drive system with fixed switching frequency," *37th IAS Annual Meeting. Conference Record of the Industry Applications Conference*, Vol. 2, pp. 837-844, Oct. 2002.

[31] C. Lascu and A. M. Trzynadlowski, "Combining the principles of sliding mode, direct torque control, and space-vector modulation in a high-performance sensorless AC drive," *IEEE Trans. Ind. Appl.*, Vol. 40, No. 1, pp. 170-177, Jan./Feb. 2004.

[32] M. R. P. Reddy, B. Brahmaiah, and T. B. Reddy, "Discrete space vector modulation algorithm based vector controlled induction motor drives for reduced ripple," *Power and Energy Systems Conference: Towards Sustainable Energy*, pp. 1-5, 2014.

[33] A. Haddoun, M. E. H. Benbouzid, D. Diallo, R. Abdessemed, J. Ghouili, and K. Srairi, "A loss-minimization DTC scheme for EV induction motors," *IEEE Trans. Veh. Technol.*, Vol. 56, No. 1, pp. 81-88, Jan. 2007.

[34] P. Vas, *Sensorless Vector and Direct Torque Control*, Oxford University Press, 1998.

[35] N. T. West and R. D. Lorenz, "Digital implementation of stator and rotor flux-linkage observers and a stator-current observer for deadbeat direct torque control of induction machines," *IEEE Trans. Ind. Appl.*, Vol. 45, No. 2, pp. 729-736, Mar./Apr. 2009.

[36] N. Schofield, "Fundamentals of power-train design for all- and hybrid-electric road vehicles," *IEEE Transportation Electrification Conference and Expo (ITEC 2014)*, pp. 1-198, Jun. 2014.

Muhterem Özgür Kızılkaya was born in Burdur, Turkey. He received his B.S. degree in electronics engineering from Gazi University, Ankara Turkey and his M.S. degree in electronics engineering from Middle East Technical University, Ankara, Turkey. He worked as a research engineer in the Turkish Air Force Aircraft upgrade programs. He is currently conducting research on power electronics and AC motor control in the Ph.D. program of Turkish Air Force Academy, Istanbul, Turkey. His current research interests include control of electric motors and active EMI filters in motor applications.

Kayhan Gülez has been an associate professor of the course Control and Automation Engineering at Yildiz Technical University since 2010. He received his B.S., M.S., and Ph.D. degrees in electrical engineering from Yildiz Technical University, Istanbul, Turkey. He worked at the Department of Electrical Engineering, Yildiz Technical University, between 1997 and 2010. He worked as a research associate in a JSPS project and other short-term projects at Keio University and Tokyo Metropolitan Institute of Technology between 1999 and 2002. His major research interests are electrical vehicle and unmanned air vehicle applications, intelligent-based control systems, sensor network control problems, EMC and EMI control methods, active, passive, and EMI filter design methods, and applications for EMI noise and harmonic problems, in which he has published and presented over 250 scientific papers and technical reports in various journals and conference proceedings. He is a reviewer and program committee member of numerous journals and conferences in these areas. He also received 13 science grand awards between 1998 and 2015 and the Superior Success Science Award in 2009 from Yildiz Technical University in Istanbul, as well as Best Paper awards from SCI'2001, M&S'2001, and TOK 2009 conferences.